Quasiparticle band structure of AlN and GaN

Angel Rubio, Jennifer L. Corkill, Marvin L. Cohen, Eric L. Shirley, and Steven G. Louie
Department of Physics, University of California at Berkeley, Berkeley, California 94720
and Materials Sciences Division, Lawrence Berkeley Laboratory, Berkeley, California 94720
(Received 5 May 1993)

The *ab initio* pseudopotential method within the local-density approximation and the quasiparticle approach have been used to investigate the electronic properties of AlN and GaN in the wurtzite and zinc-blende structures. The quasiparticle band-structure energies are calculated using a model dielectric matrix for the evaluation of the electron self-energy. For this calculation, good agreement with the experimental results for the minimum band gaps in the wurtzite structure is obtained. In the zinc-blende structure we predict that AlN will be an indirect (Γ to X) wide band-gap semiconductor (4.9 eV) and that GaN will have a direct gap of 3.1 eV at Γ in good agreement with recent absorption experiments on cubic GaN (3.2–3.3 eV). A discussion of the direct versus indirect gap as well as other differences in electronic structure between the wurtzite and zinc-blende phases is presented. Other properties of quasiparticle excitations are predicted in this work and remain to be confirmed by experiment.

I. INTRODUCTION

The III-V nitrides have attracted extensive experimental[1–5] and theoretical[6–11] interest because of the large magnitude of the forbidden gap ($E_g > 3$ eV), considerable hardness, and high thermal conductivity. Nitride semiconductors are potentially useful as high-frequency, microwave, and short-wavelength (green, blue, and ultraviolet) electroluminescent devices. The specific role of nitrogen is in the formation of short bonds which leads to smaller lattice constants (by $\sim 20\%$) than for other III-V semiconductors. Because these compounds have small atomic volumes, many of their physical properties will be similar to other wide gap semiconductors such as diamond or BN. At ambient conditions both AlN and GaN crystallize in the hexagonal wurtzite structure, but the zinc-blende structure is only slightly higher in energy (in BN the ordering of energy is reversed).[12] Under high pressure these nitride compounds undergo a structural phase transformation to the rocksalt structure (AlN at 12.9 GPa and GaN at 47 GPa)[3–5] that is favored by their high ionicity.[13,14] No transition to the zinc-blende structure is observed.

Experimental data on the microscopic parameters and electronic properties of AlN and GaN have been scarce due to the difficulties in growing high-quality single crystals. Recently, however, high quality single crystals of GaN in the wurtzite and zinc-blende structures have been epitaxially grown on Si(001) by electron cyclotron resonance microwave-plasma-assisted molecular-beam epitaxy (MBE), using a two-step growth process, in which a GaN buffer is grown at relatively low temperatures and the rest of the film is grown at higher temperatures.[1] Films of GaN grown on a single crystalline GaN buffer have the zinc-blende structure, while those grown on a polycrystalline or amorphous buffer have the wurtzite structure. Also the wurtzite structure is favored when grown on sapphire and Si(111). These and other substrates have been used in growing high quality films of GaN, AlN, and layered AlN/GaN films by MBE (Ref. 2) but most favor the wurtzite phase. Cubic GaN is interesting partly because of its potential for a higher saturated electron drift velocity and a somewhat lower band gap than wurtzite GaN.[1,2]

Calculations using the local density approximation (LDA) to the density functional theory[15] are very reliable for structural parameters (few percent error in the lattice constants, bulk moduli, and pressure-induced phase transitions) but this method lacks justification when applied to excitation energies in a crystal.[15,16] However, the LDA ground state calculations constitute a very good starting point for quasiparticle self-energy calculations because of the closeness of LDA and quasiparticle wave functions.[17] It is possible to calculate accurately from first principles the quasiparticle energies and band gaps of semiconductor and insulators[17,18] and metal[19] bulk systems as well as surfaces, interfaces, and superlattices[20] by using the so-called *GW* approximation for calculating the electron self-energy Σ.[21] The *GW* approach has resulted in calculated band gaps with 0.1 eV accuracy[17] when a random-phase approximation dielectric matrix is used, or within 0.1–0.3 eV when an appropriate model dielectric matrix is used.[17,22] This is a suitable method to predict the electronic excitations in the system that can be compared with experiments.

In this paper we study the band structure and quasiparticle excitation energies of AlN and GaN semiconductors in both the wurtzite and zinc-blende structures, focusing on the differences in electronic structure between these crystalline phases as well as between the behavior of Al and Ga in these compounds. The LDA results and those from quasiparticle *GW* calculations are compared

with the existing experimental data. The full theoretical data are tabulated for reference. The paper is organized as follows. Section II outlines the theoretical method and some numerical details. In Sec. III we present the calculated LDA and *GW* band structures for the two nitrides in both the wurtzite and zinc-blende structures. A summary is given in Sec. IV.

II. THEORY AND TECHNICAL DETAILS

First, we employ the standard plane-wave pseudopotential total-energy scheme[23] in the LDA approximation to describe the ground state. *Ab initio* semirelativistic pseudopotentials[24,25] are used. The Al and Ga ionic pseudopotentials have been generated by the Hamann-Schlüter-Chiang method[24] and the soft-pseudopotential method of Troullier and Martins[25] has been used to describe nitrogen in order to minimize the plane-wave basis set needed to describe this deeper potential. In the case of Ga the shallow $3d$-core electrons overlap significantly with the valence charge density. To describe this effect without explicitly including the d electrons as part of the valence complex we have included partial core corrections for exchange and correlation.[26] The importance of this core correction in the structural properties of gallium compounds has been shown in Ref. 27. The LDA wave functions were expanded up to a 40-Ry cutoff where good convergence in electronic eigenvalues was achieved.

To study the quasiparticle excitation energies we need to go beyond the LDA approximation. (The one-particle eigenvalues in the LDA theory have no formal justification as quasiparticle energies although, in practice, these eigenvalues have been used to discuss the spectra of solids.) Within the context of the one-particle Green's function approach we have a rigorous formulation of the quasiparticle properties. In this framework the wave function and eigenvalue of a quasiparticle in a crystal are obtained by solving the Dyson equation

$$(T + V_{\text{ext}} + V_H)\Psi_{n\mathbf{k}}(\mathbf{r}) + \int d\mathbf{r}'\Sigma(\mathbf{r},\mathbf{r}';E_{n\mathbf{k}})\Psi_{n\mathbf{k}}(\mathbf{r}) = E_{n\mathbf{k}}\Psi_{n\mathbf{k}}(\mathbf{r}), \quad (1)$$

where T is the kinetic energy operator, V_{ext} is the external potential due to the ions, V_H is the Hartree potential of the electrons, and Σ is the electron self-energy operator which contains the many-body effects of exchange and correlation between electrons and in general is a nonlocal, energy dependent, and non-Hermitian operator. In the *GW* approximation[21] Σ becomes

$$\Sigma(\mathbf{r},\mathbf{r}';E) = \frac{i}{2\pi}\int d\omega\, e^{-i\delta\omega}G(\mathbf{r},\mathbf{r}',E-\omega)W(\mathbf{r},\mathbf{r}',\omega), \quad (2)$$

where G is the dressed Green's function, W is the dynamical screened Coulomb interaction, and δ is a positive infinitesimal. Vertex corrections are not included in this approximation.[21]

In this work, the Hybertsen-Louie[17] scheme is used to calculate the electron self-energy. For the calculation of the Green's function G we make two approximations: first, an infinite lifetime for the quasiparticle is assumed and, second, the LDA eigenfunctions are taken as a good description of the quasiparticle wave functions.[17,18] The screened Coulomb interaction in Eq. (2) is given by $W = \varepsilon^{-1}V$ with V the bare Coulomb interaction. Typically the static dielectric response matrix is obtained by either a model or a linear-response perturbation calculation in the random-phase approximation.[17] Here we use a generalized form of the static Levine-Louie model dielectric function.[22,28] This model incorporates the correct limiting cases of the long-range and short-range behavior of the response function. The static dielectric matrix is extended to finite frequencies by a generalized plasmon-pole model[17] using exact sum rules to fix the frequencies and strengths of the poles in the inverse dynamical dielectric matrix elements $\varepsilon^{-1}_{\mathbf{G}\mathbf{G}'}(\omega)$.[22] This method has been successfully applied to the study of electronic excitations in a large number of semiconductors.[22,29] The model requires only the dielectric constant ε_∞ of the material as input. In principle this can be evaluated from *ab initio* calculations, but we use the experimental values[30] in this work.

There are two effects included in the *GW* approximation that are absent in the LDA calculations: the nonlocality of the screened interaction (including the local field effects of the dielectric matrix) and the energy dependence of the self-energy operator. The quasiparticle energy can be described as the LDA energy eigenvalue plus a many-body correction,

$$E_{n\mathbf{k}} = \varepsilon^{\text{LDA}}_{n\mathbf{k}} + \langle n\mathbf{k} \mid \Sigma(E_{n\mathbf{k}}) - V^{\text{LDA}}_{\text{xc}} \mid n\mathbf{k}\rangle, \quad (3)$$

where $V^{\text{LDA}}_{\text{xc}}$ is LDA exchange-correlation potential and $\mid n\mathbf{k}\rangle$ is the LDA wave function at $\mathbf{k}$ of band n. In writing Eq. (3) we have assumed again that the quasiparticle wave function is very close to its LDA counterpart.[17,18] The self-consistent quasiparticle spectrum from Eq. (1) is required in the calculation of the Green's function. In practice, it is sufficient if only the input quasiparticle energies are obtained from the conduction and valence

TABLE I. Experimental lattice constants for the wurtzite (WZ) and zinc-blende (ZB) structures, and static dielectric constants used in the quasiparticle calculations. The theoretical LDA lattice parameters are given in parentheses.

	a_{WZ} (Å)	c_{WZ} (Å)	u_{WZ}	a_{ZB} (Å)	ε_∞
AlN	3.110[a]	4.980[a]	0.382[a]	4.35[b]	4.84[d]
	(3.129)[e]	(4.988)[e]	(0.382)[e]		
GaN	3.160[a]	5.125[a]	0.377[a]	4.50[c]	5.20[d]
	(3.126)[e]	(5.119)[e]	(0.377)[e]	(4.42)[e]	

[a]Experimental data from Ref. 30.
[b]This work: theoretical *ab initio* total energy LDA calculation.
[c]Experimental data from Ref. 1.
[d]From refractive index in Ref. 30.
[e]Theoretical data from Refs. 6 and 7.

bands by linearly fitting the LDA spectrum to the calculated *GW* spectrum from a previous iteration.[29]

In the calculation of the many-body contribution to Σ several numerical cutoffs are involved.[17,22] The dielectric matrix is truncated at $|\mathbf{q}+\mathbf{G}| = 4$ a.u. We have included 10 (14) $\mathbf{k}$ points in the irreducible wedge of the Brillouin zone and 100 (150) bands in the calculation of the matrix elements of Σ in summing over the immediate scattering states for the zinc-blende (wurtzite) structure. This gives quasiparticle energies converged to about 0.1 eV.[22]

III. RESULTS

The ground-state LDA calculations have been performed at both the theoretical and experimental lattice constants[30] for the wurtzite structure of AlN and GaN and for the zinc-blende structure of GaN. Since no experimental lattice constant for zinc-blende AlN is available, the theoretical lattice constant alone is used throughout this study. The LDA band structures presented below are calculated at the theoretical lattice constant representing the LDA ground state.[31] The *GW* approach, however, should in principle be applied to the system at the experimental lattice constant. Thus all the *GW* results are quoted for the experimental unit cell volume. As the calculated and experimental volumes for these compounds differ at most by a few percent, the LDA eigenvalues are very close for the two and the distinction is simply one of technical rigor. Table I gives the values for lattice constants and static dielectric constants used in the calculations. Comparisons to previous LDA theoretical lattice constants[6,7] and experimental[1,30] ones show good

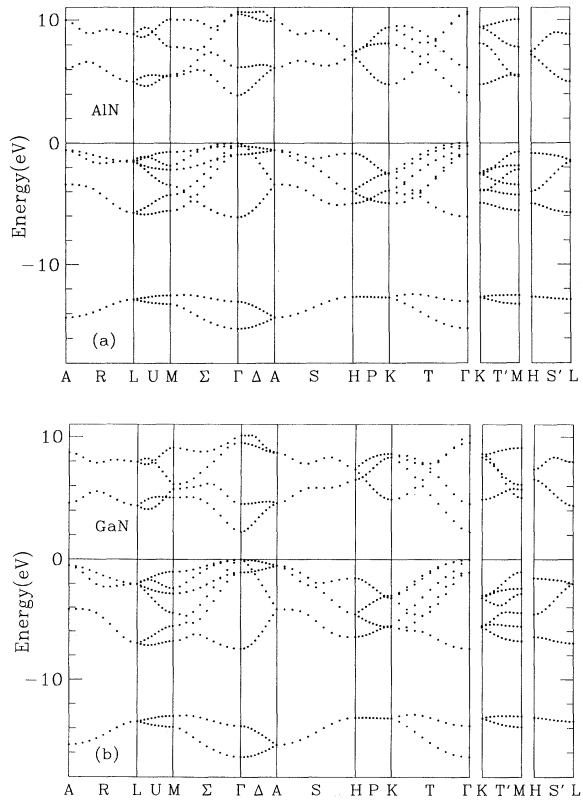

FIG. 1. LDA band-structure calculation for the wurtzite phase at the theoretical lattice constant for (a) AlN and (b) GaN.

TABLE II. AlN eigenvalues in eV for the valence bands and four conduction bands at high-symmetry points in the LDA and *GW* calculations for the wurtzite structure. All values are in reference to the valence-band maximum. The L, H, and A points shown are doubly degenerate.

	LDA	*GW*		LDA	*GW*		LDA	*GW*
Γ_1^v	-15.2	-17.4	K_3^v	-12.7	-14.8	M_1^v	-13.2	-15.4
Γ_3^v	-13.0	-15.2	K_3^v	-12.7	-14.8	M_3^v	-12.5	-14.6
Γ_3^v	-6.1	-6.9	K_1^v	-4.9	-5.6	M_1^v	-5.6	-6.3
Γ_5^v	-0.9	-1.1	K_3^v	-3.9	-4.5	M_3^v	-4.3	-4.9
Γ_5^v	-0.9	-1.1	K_3^v	-3.9	-4.5	M_1^v	-3.4	-4.0
Γ_6^v	-0.3	-0.2	K_2^v	-2.5	-3.0	M_2^v	-2.2	-2.6
Γ_6^v	-0.3	-0.2	K_3^v	-2.5	-2.9	M_3^v	-1.8	-2.1
Γ_1^v	0.0	0.0	K_3^v	-2.5	-2.9	M_4^v	-0.7	-0.9
Γ_1^c	3.9	5.8	K_2^c	4.8	6.7	M_1^c	5.5	7.4
Γ_3^c	6.2	8.3	K_1^c	8.1	10.7	M_3^c	5.6	7.6
Γ_1^c	10.5	13.4	K_3^c	9.4	12.0	M_3^c	7.8	10.1
Γ_6^c	10.6	12.9	K_3^c	9.4	12.0	M_1^c	10.0	12.9
$L_{1,3}^v$	-12.9	-15.0	$H_{1,3}^v$	-12.6	-14.8	$A_{1,3}^v$	-14.3	-16.5
$L_{1,3}^v$	-5.7	-6.5	H_3^v	-5.0	-5.6	$A_{1,3}^v$	-3.4	-3.9
$L_{2,4}^v$	-1.5	-1.8	$H_{1,2}^v$	-4.0	-4.6	$A_{5,6}^v$	-0.6	-0.7
$L_{1,3}^v$	-1.4	-1.7	H_3^v	-0.8	-1.0	$A_{5,6}^v$	-0.6	-0.7
$L_{1,3}^c$	5.0	6.9	H_3^c	7.2	9.5	$A_{1,3}^c$	6.1	8.3
$L_{1,3}^c$	8.9	11.1	$H_{1,2}^c$	7.5	9.6	$A_{5,6}^c$	10.0	12.5

TABLE III. GaN eigenvalues in eV for the valence bands and four conduction bands at high-symmetry points in the LDA and *GW* calculations for the wurtzite structure. All values are in reference to the valence-band maximum. The L, H, and A points shown are doubly degenerate.

	LDA	*GW*		LDA	*GW*		LDA	*GW*
Γ_1^v	-16.3	-18.2	K_3^v	-13.2	-15.2	M_1^v	-13.9	-15.8
Γ_3^v	-13.8	-15.7	K_3^v	-13.2	-15.2	M_3^v	-13.0	-15.0
Γ_3^v	-7.4	-8.0	K_1^v	-5.6	-6.1	M_1^v	-6.8	-7.4
Γ_5^v	-1.1	-1.2	K_3^v	-5.5	-6.1	M_3^v	-5.6	-6.1
Γ_5^v	-1.1	-1.2	K_3^v	-5.5	-6.1	M_1^v	-4.4	-4.9
Γ_1^v	0.0	0.0	K_3^v	-3.2	-3.5	M_2^v	-2.8	-3.1
Γ_6^v	0.0	0.0	K_3^v	-3.2	-3.5	M_3^v	-2.4	-2.6
Γ_6^v	0.0	0.0	K_2^v	-3.0	-3.2	M_4^v	-1.0	-1.1
Γ_1^c	2.3	3.5	K_2^c	4.9	6.6	M_1^c	5.1	6.5
Γ_3^c	4.6	5.9	K_3^c	8.3	10.6	M_3^c	5.7	7.4
Γ_1^c	9.5	12.1	K_3^c	8.3	10.6	M_3^c	6.2	8.1
Γ_6^c	10.1	11.9	K_1^c	8.6	10.8	M_1^c	9.1	11.5
$L_{1,3}^v$	-13.4	-15.4	$H_{1,3}^v$	-13.1	-15.1	$A_{1,3}^v$	-15.4	-17.2
$L_{1,3}^v$	-7.0	-7.6	H_3^v	-6.4	-7.1	$A_{1,3}^v$	-4.1	-4.6
$L_{2,4}^v$	-2.0	-2.2	$H_{1,2}^v$	-4.6	-4.9	$A_{5,6}^v$	-0.5	-0.6
$L_{1,3}^v$	-2.0	-2.2	H_3^v	-1.5	-1.6	$A_{5,6}^v$	-0.5	-0.6
$L_{1,3}^c$	4.4	6.0	H_3^c	6.6	8.3	$A_{1,3}^c$	4.6	6.1
$L_{1,3}^c$	8.0	9.9	$H_{1,2}^c$	7.4	9.4	$A_{5,6}^c$	8.7	10.8

agreement. Similar agreement will be expected for the zinc-blende phase of AlN.

The LDA band structures for AlN and GaN in the wurtzite phase are given in Figs. 1(a) and 1(b), respectively. These results agree well with previous theoretical calculations which use the full-potential linear-muffin-tin orbital (FLMTO) method and include the gallium d-core electrons as part of the valence electrons.[11] This shows that by including the partial core corrections, we get a fairly good description of the effect of the d-core electrons on the valence complex within the context of density functional theory.[27] Compared to other plane-wave calculations which were done at a lower cutoff energy, we systematically obtain larger gaps [the largest differences are 0.9 eV at the Γ point in AlN (Ref. 6) and 0.6 eV at Γ in GaN (Ref. 7)]. The larger cutoff used here is needed to obtain converged eigenfunctions and eigenvalues to be used as input for the quasiparticle calculations. No significant change is seen in our work by increasing the cutoff further to 80 Ry. The order of the levels at the top of the valence band, Γ_6^v and Γ_1^v, is inverted in AlN with respect to GaN. The difference between these levels is 0.2 eV in AlN and 0.02 eV in GaN. Due to the hexagonal symmetry of these compounds, the top of the valence band is split into two levels, in contrast to the zinc-blende compounds where the top of the valence band is triply degenerate.

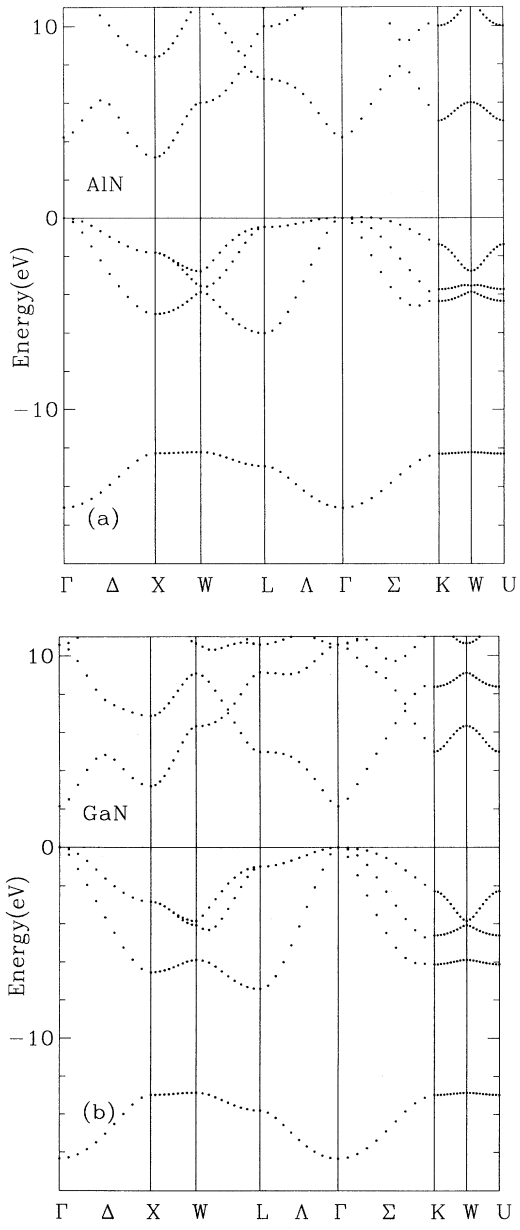

FIG. 2. LDA band structure calculation for the zinc-blende phase at the theoretical lattice constant for (a) AlN and (b) GaN.

TABLE IV. AlN eigenvalues in eV at high-symmetry points in the LDA and *GW* calculations for the zinc-blende structure. All values are in reference to the valence-band maximum. The *GW* calculation here is done at the theoretical lattice constant.

	LDA	*GW*		LDA	*GW*		LDA	*GW*
Γ_1^v	-15.1	-17.0	L_1^v	-12.9	-14.9	X_1^v	-12.3	-14.3
Γ_{15}^v	0.0	0.0	L_1^v	-6.0	-6.7	X_3^v	-5.0	-5.6
Γ_{15}^v	0.0	0.0	L_3^v	-0.5	-0.6	X_5^v	-1.8	-2.1
Γ_{15}^v	0.0	0.0	L_3^v	-0.5	-0.6	X_5^v	-1.8	-2.1
Γ_1^c	4.2	6.0	L_1^c	7.3	9.3	X_1^c	3.2	4.9
Γ_{15}^c	12.3	14.6	L_1^c	10.0	12.6	X_1^c	8.4	10.5
Γ_{15}^c	12.3	14.6	L_3^c	11.0	13.2	X_3^c	14.1	17.3
Γ_{15}^c	12.3	14.6	L_3^c	11.0	13.2	X_5^c	15.7	18.7

The eigenvalues from the LDA and *GW* calculations for AlN and GaN in the wurtzite structure are listed in Tables II and III for six high symmetry points of the Brillouin zone. All energies are in reference to the top of the valence band (Γ_1^v), and their symmetries are indicated following Ref. 32. The *GW* excitation energies do not significantly alter the main physical effects given by the LDA calculation, but the magnitude of the gaps and the valence and conduction bandwidths are both increased by $\sim$ 1–2 eV. As in the case of diamond and other wide gap semiconductors like BN,[29] the strong local field effect produces a **k**-directional dependence on the many-body correction to the LDA eigenvalues for AlN and GaN. That is, in the wurtzite structure the *GW* band gap is larger than the LDA band gap at the experimental lattice constant by 1.8 (1.4) eV at Γ, while the

TABLE V. GaN eigenvalues in eV at high-symmetry points in the LDA and *GW* calculations for the zinc-blende structure. All values are in reference to the valence-band maximum.

	LDA	*GW*		LDA	*GW*		LDA	*GW*
Γ_1^v	-16.3	-17.8	L_1^v	-13.8	-15.5	X_1^v	-13.0	-14.8
Γ_{15}^v	0.0	0.0	L_1^v	-7.4	-7.8	X_3^v	-6.5	-6.9
Γ_{15}^v	0.0	0.0	L_3^v	-1.0	-1.1	X_5^v	-2.8	-3.0
Γ_{15}^v	0.0	0.0	L_3^v	-1.0	-1.1	X_5^v	-2.8	-3.0
Γ_1^c	2.1	3.1	L_1^c	5.0	6.2	X_1^c	3.2	4.7
Γ_{15}^c	10.6	12.2	L_1^c	9.1	11.2	X_1^c	6.9	8.4
Γ_{15}^c	10.6	12.2	L_3^c	10.6	12.3	X_3^c	12.2	14.5
Γ_{15}^c	10.6	12.2	L_3^c	10.6	12.3	X_5^c	14.6	16.7

gap at H is larger by 2.3 (1.8) eV for AlN (GaN).

In Figs. 2(a) and 2(b) the LDA band structures for AlN and GaN in the zinc-blende phase are given. As in the wurtzite band structures, the overall features of these bands agree well with previous calculations using localized basis functions.[9,11] Again for cubic GaN a larger band gap is found when compared to other plane-wave calculations[7] (an increase of 0.6 eV at Γ). In Tables IV and V the results of the LDA and *GW* calculations are listed for the zinc-blende structure. The main difference between the two materials is that AlN is an indirect semiconductor (Γ to X) similar to BN,[29] while GaN is direct at Γ. This effect is also observed in the widely used III-V semiconductors AlAs and GaAs where the aluminum compound is indirect while the gallium compound is direct. In the zinc-blende structure the *GW* many-body correction has a **k**-directional dependence shown in an increase of the gap in AlN (GaN) by 1.8 (1.4) eV at Γ and by 2.0 (1.6) eV at L, similar to the **k**-directional dependence found in BN.[29] As for the wurtzite structure, the main physical effects on the quasiparticle levels are included in the LDA counterpart. It is important to note that the assumption of infinite lifetimes for the quasiparticles within the *GW* framework generally leads to a less reliable description of the higher-energy excitations since it is invalid for excitation energies much greater than the gap. At present, we treat core-valence exchange and correlation at an LDA level only, and we neglect core relaxation effects which could be important for materials with shallow cores.[33] Whereas we plan to investigate these effects further in future work, we anticipate that the results in this work will not be significantly changed (note that our pseudopotential band calculation agrees well with FLMTO calculation including the core electrons in the valence complex).

Comparing AlN and GaN in both wurtzite and zinc-blende structures, we observe that, even though the lattice mismatch is small, the electronic properties are quite different. Namely, GaN has generally smaller band gaps than AlN in both wurtzite and zinc-blende structures and in the zinc-blende phase AlN is an indirect band gap semiconductor whereas GaN is direct. Changes in the relative positions of the conduction band levels with respect to the top of the valence band are large for conduction band levels having some s character on the cation (as in the case of the Γ point). The difference in the Al and Ga pseudopotentials can be used to explain these changes.[34]

To understand these materials better, we have analyzed the differences in the band structure of the wurtzite and zinc-blende phases. Using the projection of the symmetry points and lines zone of the zinc-blende structure onto the hexagonal zone given in Ref. 32, we can compare the two band structures. In Tables VI and VII this comparison is made for AlN and GaN. Due to the similarities in the atomic arrangement in the zinc-blende and wurtzite structures (both have tetrahedral bonds, contain six-membered rings of bonds, and only differ in the second-nearest neighbors), their electronic properties, in particular the width of the valence and conduction complexes as well as the energy gaps at high symmetry points, are quite similar (see also Figs. 1 and 2).

An important difference is that AlN changes from a direct gap semiconductor to indirect in going from wurtzite to zinc-blende. This difference comes from a change in the relative position of the X_1^c point. To understand this behavior we can look at the symmetry and the angular decomposition of the X_1^c point in the two structures. In the zinc-blende this state has mainly s character at the anion and p character at the cation and the only state with the same symmetry is the X_1^v which is far away in energy. The corresponding point in the wurtzite structure[35] has a lower symmetry and thus can interact with several closer lying states that will tend to push this level upwards. In addition, the state now has less s character on the anion and more on the cation. Because the nitrogen has a more attractive atomic potential than the corresponding cation and the larger the s character on the anion the lower the energy of the level, we can expect that the transfer of s character will also shift the level upwards. These two effects together can qualitatively be used to explain why this level is at a higher energy in the wurtzite structure than in the zinc-blende for both AlN and GaN. Because the character at the top of the valence band and bottom of the conduction band (Γ point) is nearly the same in both structures we can use the previous argument to explain why the gap at Γ doesn't change as much. The fact that the type of gap differs in wurtzite and zinc-blende for AlN and not for GaN is connected to the inherent size of the gap at Γ and is due to the differences in the nonlocal angular

TABLE VI. AlN gaps and bandwidths from LDA and *GW* methods for the wurtzite and zinc-blende structures. The experimental gap for wurtzite is given for comparison.

	Wurtzite				Zinc-blende	
	LDA	*GW*	Expt.		LDA	*GW*
$E_g(\Gamma_1^v \to \Gamma_1^c)$	3.9	5.8	6.2[a]	$\Gamma_{15}^v \to \Gamma_1^c$	4.2	6.0
$\Gamma_1^v \to$ "X_1^c" [b]	4.7	6.4		$E_g(\Gamma_{15}^v \to X_1^c)$	3.2	4.9
Antisymmetric gap	6.3	7.7			6.3	7.6
Upper-valence bandwidth	6.1	6.9			6.0	6.7
Total-valence bandwidth	15.2	17.4			15.1	17.0

[a]Optical absorption from Ref. 30.

[b]Here, X refers to the point in the wurtzite Brillouin zone equivalent to the X point in the zinc-blende zone (Ref. 32).

TABLE VII. GaN gaps and bandwidths from LDA and *GW* methods for the wurtzite and zinc-blende structures. Experimental band gaps are given for comparison.

	Wurtzite				Zinc-blende		
	LDA	*GW*	Expt.		LDA	*GW*	Expt.
$E_g(\Gamma_6^v \rightarrow \Gamma_1^c)$	2.3	3.5	3.5[a]	$E_g(\Gamma_{15}^v \rightarrow \Gamma_1^v)$	2.1	3.1	3.2,[b]3.3[c]
$\Gamma_6^v \rightarrow$ "X_1^c" [d]	4.1	5.6		$\Gamma_{15}^v \rightarrow X_1^c$	3.2	4.7	
Antisymmetric gap	5.4	7.0			5.6	7.0	
Upper-valence bandwidth	7.4	8.0			7.4	7.8	
Total-valence bandwidth	16.3	18.2			16.3	17.8	

[a]Photoluminescence from Ref. 30.
[b]Optical absorption from Ref. 1.
[c]Photoluminescence and cathodoluminescence from Ref. 2.
[d]Here, X refers to the point in the wurtzite Brillouin zone equivalent to the X point in the zinc-blende zone (Ref. 32).

components of the Al and Ga pseudopotentials.[34]

As shown in Tables VI and VII the value of the antisymmetric gap is larger in AlN than in GaN for both structures. Since this gap is related to the ionicity of the semiconductor,[13] we obtain that AlN is a slightly more ionic material than GaN in agreement with the ionicity scale of Ref. 14. The fact that AlN has a lower pressure phase transition to the rocksalt structure in spite of its slightly higher ionicity is most likely related to the effect of the Ga d-core electrons on the structural properties. From the wurtzite and zinc-blende LDA band structures we can estimate the average conduction-valence gap, E_g, to be $\sim$ 7.8 eV for AlN and $\sim$ 7.1 eV for GaN.

There are several main effects of the many-body *GW* quasiparticle corrections to the Kohn-Sham eigenvalue band structure. First the minimum band gap is increased by nearly 40% leading to good agreement with the available experimental data. The total valence bandwidth is increased by $\sim$2 eV and the "upper" valence bandwidth (bands 3–8) by $\sim$ 0.7 eV. Roughly speaking, the LDA conduction band is rigidly shifted upwards and then broadened by $\sim$ 20%. This will change the average gap E_g to 11.2 eV for AlN and 10.1 eV for GaN. If we put the experimental dielectric constant[30] into the Phillips[13] dielectric model of the chemical bond, $\varepsilon = 1+(\hbar\omega_p/E_g)^2$, where ω_p is the theoretical bulk plasma frequency, we obtain E_g=11.6 eV for AlN and 10.8 eV for GaN in good agreement with our quasiparticle estimation and with the empirical values of Phillips of 11 eV for AlN and 10.8 eV for GaN.[13]

Due to the lack of experimental data for the zinc-blende structure of AlN we have performed the calculation of the *GW* quasiparticle energies at the calculated LDA lattice constant. We find that cubic AlN will be a wide gap indirect (Γ to X) semiconductor with a minimum band gap of 4.9 eV. The use of the theoretical lattice constant instead of the experimental one could lead to an error of 0.3 eV (Ref. 36) in the predicted gap for cubic AlN. We predict that cubic GaN has a direct gap of 3.1 eV at Γ.

IV. CONCLUSIONS

An accurate description of the band structure and excitation energies of the wide gap nitrides, AlN and GaN, has been obtained by calculating the self-energy operator within the *GW* approximation. Good agreement with available experimental data has been found. We have studied the difference in electronic properties between these compounds in both the wurtzite and zinc-blende structure. AlN and GaN in the zinc-blende structure are found to have wide energy gaps comparable to the corresponding wurtzite gaps. However, in the zinc-blende structure, AlN is predicted to be indirect with a gap of about 4.9 eV, while cubic GaN is found to be direct with a gap of about 3.1 eV. We have given a qualitative explanation for these changes based on the symmetry and angular character of the different conduction-band states (at Γ and X). Furthermore, since there are no available experimental excitation energies other than the minimum band gap, the theoretical results contained in Tables II–VII are presently the best available estimates known to us for the electronic excitations of these wide gap nitride semiconductors.

ACKNOWLEDGMENTS

This work was supported by National Science Foundation Grant No. DMR91-20269 and by the Director Office of Energy Research, Office of Basic Energy Sciences, Materials Sciences Division of the U.S. Department of Energy under Contract No. DE-AC03-76SF00098. Cray Computer time was provided by the National Science Foundation at the Pittsburgh Supercomputing Center. A.R. was supported by a Fullbright-MEC grant. J.L.C. acknowledges support from AT&T Bell Laboratories. E.L.S. is supported by the Miller Institute for Basic Research in Science.

[1] T. Lei, T.D. Moustakas, R.J. Graham, Y. He, and S.J. Berkowitz, J. Appl. Phys. **71**, 4933 (1992); T. Lei, M. Fanciulli, R. J. Molnar, T.D. Moustakas, R.J. Graham, and J. Scanlon, Appl. Phys. Lett. **59**, 944 (1992); C.R. Eddy, T.D. Moustakas, and J. Scanlon, J. Appl. Phys. **73**, 448 (1993).

[2] M.J. Paisley, Z. Sitar, J.B. Posthill, and R.F. Davis, J. Vac. Sci. Technol. A **7**, 701 (1989); Z. Sitar *et al.*, J. Mater. Sci. Lett. **11**, 261 (1992).

[3] P. Perlin, C. Jauberthie-Carillon, J.P. Itie, A. San Miguel, I. Gorczyca, and A. Polian, Phys. Rev. B **45**, 83 (1992); P. Perlin, I. Gorczyca, N.E. Christensen, I. Grzegory, H. Teisseyre, and T. Suski, *ibid.* **45**, 13 307 (1992).

[4] H. Vollstädt, E. Ito, M. Akaishi, S. Akimoto, and O. Fukunaga, Proc. Jpn. Acad. B **66**, 7 (1990).

[5] M. Ueno, A. Onodera, O. Shimomura, and K. Takemura, Phys. Rev. B **45**, 10 123 (1992).

[6] P.E. Van Camp, V.E. Van Doren, and J.T. Devreese, Phys. Rev. B **44**, 9056 (1991).

[7] P.E. Van Camp, V.E. Van Doren, and J.T. Devreese, Solid State Commun. **81**, 23 (1992).

[8] A. Muñoz and K. Kunc, Phys. Rev. B **44**, 10 372 (1991).

[9] W.Y. Ching and B.N. Harmon, Phys. Rev. B **34**, 5305 (1986).

[10] V. Fiorentini, M. Methfessel, and M. Scheffler, Phys. Rev. B **47**, 13 353 (1993).

[11] W.R.L. Lambrecht and B. Segall, in *Wide Band-Gap Semiconductors*, edited by T.D. Moustakas, J.I. Pankove, and Y. Hamakawa, MRS Symposia Proceedings No. 242 (Materials Research Society, Pittsburgh, 1992), p. 367.

[12] R.M. Wentzcovitch, M.L. Cohen, and P.K. Lam, Phys. Rev. B **36**, 6058 (1987).

[13] J.C. Phillips, Rev. Mod. Phys. **42**, 317 (1970).

[14] A. García and M.L. Cohen, Phys. Rev. B **47**, 4215 (1993); **47**, 4221 (1993).

[15] P. Hohenberg and W. Kohn, Phys. Rev. **136**, B864 (1964); W. Kohn and L.J. Sham, *ibid.* **140**, A1133 (1965).

[16] J.P. Perdew and M. Levy, Phys. Rev. Lett. **51**, 1884 (1983); L.J. Sham and M. Schlüter, *ibid.* **51**, 1888 (1983).

[17] M.S. Hybertsen and S.G. Louie, Phys. Rev. Lett. **55**, 1418 (1985); Phys. Rev. B **34**, 5390 (1986); S.B. Zhang, D. Tománek, M.L. Cohen, S.G. Louie, and M.S. Hybertsen, *ibid.* **40**, 3162 (1989).

[18] R.W. Godby, M. Schlüter, and L.J. Sham, Phys. Rev. Lett. **56**, 2415 (1986); Phys. Rev. B **36**, 6497 (1987); **37**, 10 159 (1988).

[19] J.E. Northrup, M.S. Hybertsen, and S.G. Louie, Phys. Rev. Lett. **59**, 819 (1987).

[20] M.S. Hybertsen and S.G. Louie, Phys. Rev. Lett. **58**, 1551 (1987); Phys. Rev. B **38**, 4033 (1988); X. Zhu, S.B. Zhang, S.G. Louie, and M.L. Cohen, Phys. Rev. Lett. **63**, 2112 (1989); M.S. Hybertsen and M. Schlüter, Phys. Rev. B **36**, 9683 (1987).

[21] L. Hedin, Phys. Rev. **139**, A796 (1965); L. Hedin and S. Lundqvist, in *Solid State Physics: Advances in Research and Applications*, edited by F. Seitz, D. Turnbull, and H. Ehrenreich (Academic, New York, 1969), Vol. 23, p. 1.

[22] M.S. Hybertsen and S.G. Louie, Phys. Rev. B **37**, 2733 (1988); X. Zhu and S.G. Louie, *ibid.* **43**, 14 142 (1991).

[23] J. Ihm, A. Zunger, and M.L. Cohen, J. Phys. C **12**, 4409 (1979); W.E. Pickett, Comput. Phys. Rep. **9**, 115 (1989).

[24] D.R. Hamann, M. Schlüter, and C. Chiang, Phys. Rev. Lett. **43**, 1494 (1979).

[25] N. Troullier and J.L. Martins, Solid State Commun. **74**, 613 (1990); Phys. Rev. B **43**, 1993 (1991).

[26] S.G. Louie, S. Froyen, and M.L. Cohen, Phys. Rev. B **26**, 1738 (1982).

[27] A. García and M.L. Cohen, Phys. Rev. B **47**, 6751 (1993); B.J. Min, C.T. Chan, and K.M. Ho, *ibid.* **45**, 1159 (1992).

[28] Z.H. Levine and S.G. Louie, Phys. Rev. B **25**, 6310 (1982).

[29] M.P. Surh, S.G. Louie, and M.L. Cohen, Phys. Rev. B **43**, 9126 (1991).

[30] *Numerical Data and Functional Relationships in Science and Technology*, edited by K.H. Hellwege, Landolt-Börnstein Tables, Group III, Vol. 17a (Springer, New York, 1982).

[31] V. Fiorentini, Solid State Commun. **83**, 871 (1992).

[32] T.K. Bergstresser and M.L. Cohen, Phys. Rev. **164**, 1069 (1967); M.R. Salehpour and S. Satpathy, Phys. Rev. B **41**, 3048 (1990).

[33] E.L. Shirley, X. Zhu, and S.G. Louie, Phys. Rev. Lett. **69**, 2955 (1992), and references therein.

[34] J.L. Corkill, A. Rubio, and M.L. Cohen (unpublished).

[35] The position of the X point in the wurtzite structure is in the M-L direction, two-thirds of the distance away from M.

[36] This is an estimate based on the change in the band gap of cubic GaN between the GW calculation done at the experimental and theoretical lattice constants (see Table I).